13 Small Renal Neoplasms

Nancy S. Curry

CONTENTS

13.1 Introduction

A subset of renal parenchymal neoplasms, lesions under 3 cm in greatest diameter, presents special challenges to the radiologist, pathologist, and urologist. These lesions became significant as CT came into use because masses of this size frequently escaped the capability of standard excretory urography (EXU), even with tomography, to detect them (Amendola et al. 1988; Curry et al. 1986; Jamis-Dow et al. 1996). The relative sensitivities of EXU, ultrasound (US), and incremental (non-helical) CT for detecting renal lesions under 3 cm in diameter are 67, 79, and 94%, respectively (Warshauer et al. 1988). Before CT and US were in routine use, only 5% of renal cell carcinomas (RCC) were discovered at this small size (Smith et al. 1989). In the decade from the mid-1980s to the mid-1990s, however, the number of imaging studies performed nearly doubled, with the result that one-half to two-thirds of small RCCs are now detected incidentally on cross-sectional imaging (Hsu et al. 2004; Volpe et al. 2004).

N. S. Curry, MD
Professor of Radiology and Urology, Department of Radiology, Medical University of South Carolina, 169 Ashley Avenue, Charleston, SC 29425, USA

13.2 Pathology

Autopsy series have shown a 7–23% incidence of renal tumors 3 cm in diameter or less (Petersen et al. 1992). The most common cause of a solid renal mass under 3 cm in diameter is RCC, accounting for about 68–90% of resected tumors of this size (Jinzaki et al. 2000; Levine et al. 1989; Silverman et al. 1994). The remainder of the lesions in these series proved to be oncocytoma, metanephric adenoma, leiomyoma, angiomyolipoma (AML), transitional cell carcinoma, and lymphoma. Oncocytomas are derived from proximal tubular cells and have finely granular, eosinophilic cytoplasm. They are difficult to distinguish from malignant tumors since oncocytes may be found in RCC. Metanephric adenoma, an uncommon but distinct type of benign renal epithelial tumor composed of small tubular structures with papillary infoldings, has been recognized and reported with increased frequency (Fielding et al. 1999; Jinzaki et al. 2000). Other non-cystic, non-neoplastic abnormalities, such as focal renal infection, infarction, malakoplakia and rare heterotopic tissue (extramedullary hematopoiesis, adrenal rests, and endometriosis), may mimic renal neoplasms.

Tumors less than 2 cm in diameter, removed during partial nephrectomy, have about one chance in three of benign pathology (Steinberg et al. 2003). Sectioning of the kidneys in a series of 500 unselected necropsies in a Portuguese population revealed that 39% contained cysts, 18% medullary fibrous nodules, 4% cortical adenomas, 1% leiomyomas, and < 1% contained lipomas, fibromyolipomas, and capsular fibromas (Reis et al. 1988). Most of these lesions were less than 1 cm in diameter.

The choice of 3 cm to define a "small" renal neoplasm is an arbitrary one, based on controversy in the pathologic literature regarding whether benign renal adenoma is a distinct entity from a small renal carcinoma. Large renal cancers have to be small at some point in their evolution, but unlike the well-known colon polyp to carcinoma progression, there is no predictable adenoma–carcinoma sequence for renal parenchymal neoplasms. Both tumors arise from the proximal convoluted tubule and pathologic features lack clear-cut criteria to differentiate them (Bennington 1973). Bell's analysis of 65 renal tumors established that the likelihood of metastases increases as the size of a renal tumor increases (Bell 1950). That series revealed only three tumors with diameters less than 3 cm (4.6%) that showed evidence of metastasis at autopsy. While some pathologists interpreted these statistics as a rationale for considering such small lesions benign, most currently classify small renal tumors as potentially malignant or pre-malignant lesions (Bennington 1973; Bennington 1987; Someren et al. 1989). Some researchers who argue that since the term "adenoma" implies a benign neoplasm, its use to describe small renal tumors should be abandoned. DNA content analysis of small renal tumors supports the hypothesis that at least some of these tumors have the potential for aggressive behavior because they demonstrate DNA aneuploidy, a feature shared by larger RCCs (Ellis et al. 1992).

Fig. 13.1. Clear cell carcinoma in a 33-year-old man with right flank pain and history of renal calculi. Axial contrast-enhanced CT scan reveals a 2.5 cm right renal enhancing solid mass (89 HU; *arrow*). A Fuhrman nuclear grade II/IV clear cell carcinoma was resected.

Fig. 13.2. Papillary RCC in a 63-year-old woman with left flank pain and hematuria. Axial contrast-enhanced CT scan reveals a homogeneous 2 cm left renal mass (83 HU; *arrow*). A partial nephrectomy was performed.

Fig. 13.3. Chromophobe RCC in a 70-year-old woman. Axial contrast-enhanced CT scan shows incidental 2.7 cm left renal mass which enhanced 71 HU over baseline scan. (With permission from Curry 2002)

13.3 Growth Characteristics

The histologic distribution of small renal carcinomas is similar to that of larger tumors, with the clear cell subtype accounting for about 70% of cases (Fig. 13.1), papillary 20% (Fig. 13.2), chromophobe 5% (Fig. 13.3), and sarcomatoid lesions occurring less frequently (Hsu et al. 2004). Most are low-grade, low-stage tumors with variable growth rates (Fig. 13.4). In Bosniak's series, 40 patients with renal neoplasms 3.5 cm in diameter or smaller were followed from 1.75 months to 8.5 years (mean 3.25 years; Bosniak et al. 1995). A mean linear growth rate of 0–1.1 cm/year (mean 0.36 cm/year) was established for these lesions and no metastases occurred in the observation period. Most of the tumors (75%) grew no more than 0.5 cm/year. Twenty-six of these tumors were resected. Most were Fuhrman grade I lesions, whereas four were

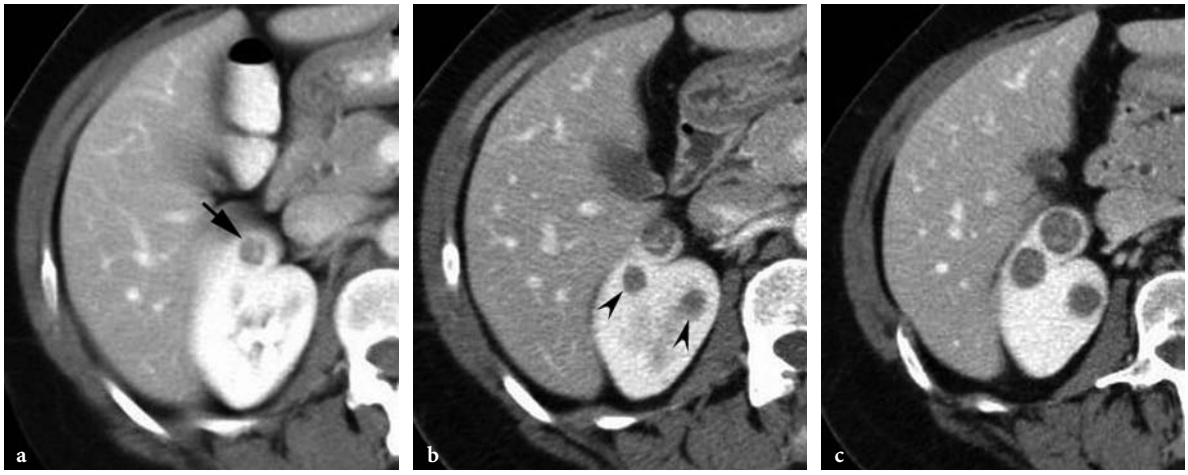

Fig. 13.4a-c. Growth of RCC in a 55-year-old woman post-left nephrectomy for clear cell carcinoma. No history of hereditary or familial renal cancer syndromes. **a** Axial contrast-enhanced CT scan shows 7 mm tumor in the anterior right kidney (*arrow*). **b** Axial contrast-enhanced CT scan 2 years later shows that the lesion grew to 12 mm in diameter and two smaller lesions appeared (*arrowheads*). **c** Axial contrast-enhanced CT scan 4 years after the first scan (**a**) shows that the anterior mass increased to 18 mm diameter. The resected lesions were all clear cell carcinoma. Additional masses were treated with radiofrequency ablation.

grade II. Even the three tumors which grew more rapidly, at 1.0–1.1 cm/year never metastasized, and two of these were grade II.

A prospective study presented the follow-up of 32 tumors in 29 patients with renal masses less than 4 cm in diameter who either refused or were unfit for surgery (Rendon et al. 2000). These patients were examined with serial abdominal imaging with US, CT, or MR imaging exams. Median follow-up was 27.9 months (range 5.3–143 months) with three or more observations per patient. Average overall growth rate was 0.1 cm/year. Five of these tumors were ultimately resected due to increases in size, and four were removed due to patient anxiety despite no change in size. Eight tumors were RCCs and one was an oncocytoma. Four of the RCCs were Fuhrman grade II, and two each were grades III and IV. Despite the fact that 11 of 32 masses (34%) doubled in volume within 1 year or achieved a diameter of 4 cm, none of the patients developed metastases or died of RCC. The authors concluded that one-third of small renal neoplasms grow under observation, but that growth is slow or undetectable in the majority. Rather than immediate surgery for small renal neoplasms, the authors proposed a period of cautious initial observation in selected patients, especially the elderly or infirm, with surgery reserved for those patients with rapid doubling times.

While the vast majority of renal tumors this size behave in a benign fashion, there have been multiple reports of metastases associated with them (Amendola et al. 1988; Bell 1950; Curry et al. 1986; Hajdu and Thomas 1967; Talamo and Shonnard 1980). Aizawa et al. (1987) reported a retrospective study of 40 RCCs under 3 cm of which 7 (17.5%) had remote metastases at surgery or autopsy. Those which metastasized were associated with a more infiltrative growth pattern, solid or alveolar microscopic structure, granular or spindle cell type, atypical nuclei, lower nephron origin, and advanced patient age. Prognosis is poor once metastases have occurred with 5-year survival in the range of 5–10%.

A study of patients with renal cancer associated with uremic acquired cystic disease showed that some high-grade tumors doubled in volume in less than 6 months, with growth most pronounced in a solid pattern, grade III sarcomatous lesion (Takebayashi et al. 2000). Due to the variable growth rate of these neoplasms, the authors recommend an initial follow-up CT at 3 months to detect the most aggressive lesions, and again at 1-year intervals. Surgical resection was recommended for lesions with volume doubling times of less than 1 year, and immediate removal of tumors with volume doubling times of less than 6 months.

In another series illustrating the potential for aggressive clinical behavior of small renal carcinomas, 5 of 74 patients (7%) with tumors under 3 cm treated by radical nephrectomy had positive nodes or distant metastases at diagnosis (Eschwege et al. 1996). A report by Hsu et al. (2004) showed that of 50 renal lesions 3 cm or smaller, 19 tumors (38%)

had extension outside the renal capsule at the time of surgery (T3 or T4) and 14 (28%) possessed a high nuclear grade (Fuhrman grade III or IV). The majority (70%) of them were clear cell carcinoma with the rest (28%) composed of papillary or chromophobe tumors. This tendency toward higher grade and stage at presentation is distinctly greater than reported in previous series.

13.4 CT Imaging

13.4.1 Technical Considerations

Multiphasic helical CT is the standard methodology of renal mass detection and characterization, with US and MR imaging playing secondary roles. Even before the development of multidetector helical scanners, 95% of renal masses 8–15 mm in diameter and 74% of lesions smaller than 8 mm were detectable (Szolar et al. 1997). The current generation of 16-slice scanners allows much faster scanning, providing very thin-section images with reconstruction capabilities that allow even earlier detection and better characterization of renal masses.

Given an adequate intravenous bolus of contrast material, even very tiny renal lesions <5 mm are clearly visible. Characterization is much more difficult than detection, however, as it is necessary to accurately distinguish small simple cysts from solid renal neoplasms. This was a particular problem before helical CT scanners became widely available in the 1990s. Renal cysts are very common in older individuals. They are usually round, homogeneous, well-defined from the adjacent parenchyma, and have no calcification or significant wall thickening. Unfortunately, some renal tumors, particularly the smaller ones, share these features. It is never safe, therefore, to assume that lesions with these characteristics are simple cysts by their appearance alone (Fig. 13.5).

An objective way of assuring that a lesion is a cyst is to place an electronic cursor within it, which is easily accomplished at the CT console or with a picture-archiving system. Simple cyst fluid registers 0–20 Hounsfield units (HU; Bosniak and Rofsky 1996). When a mass shows higher values, comparison between pre-contrast and post-contrast images is crucial to determine if there is significant enhancement of the lesion. A cyst may exhibit density greater than water on the initial scan if it has undergone internal hemorrhage. It would not be expected to change after intravenous contrast material is administered, however. An increase in density of more than 10–15 HU is considered evidence that tumoral microcirculation is distributing contrast within it (Fig. 13.6). In some cases, when a renal mass is incidentally detected on a single-phase CT performed for reasons unrelated to the kidneys, delayed images at 10 min can be obtained to see if the lesion de-enhances. Any hyperdense internal content within a hemorrhagic cyst would be expected to stay at the same density on delayed scans, whereas a neoplasm would be expected to show a decrease in density as the contrast washes out of it (Macari and Bosniak 1999).

Fig. 13.5. Papillary type clear cell carcinoma in a 41-year-old man with flank pain. Axial contrast-enhanced CT scan shows a left 2.6 cm renal mass (*arrow*) which is homogeneous and superficially resembles a simple renal cortical cyst. It measured 45 HU, however, and showed enhancement of 20 HU from baseline unenhanced CT scan (not shown). Resected tumor was a papillary-type clear cell carcinoma, Fuhrman grade II/IV.

One of the few clearly recognizable solid renal tumors on CT is AML, because the macroscopic fat content of this tumor has a characteristic negative density value (Figs. 13.7, 13.8). Even very small amounts of fat are detectable by pixel mapping. Unfortunately, in a small minority of these tumors, the muscle or angiomatous components predominate and these AMLs therefore cannot be distinguished from RCC (Fig. 13.9).

13.4.2 Lesion Pseudoenhancement

Unfortunately, the renal parenchyma surrounding a simple cyst has its own microcirculation distrib-

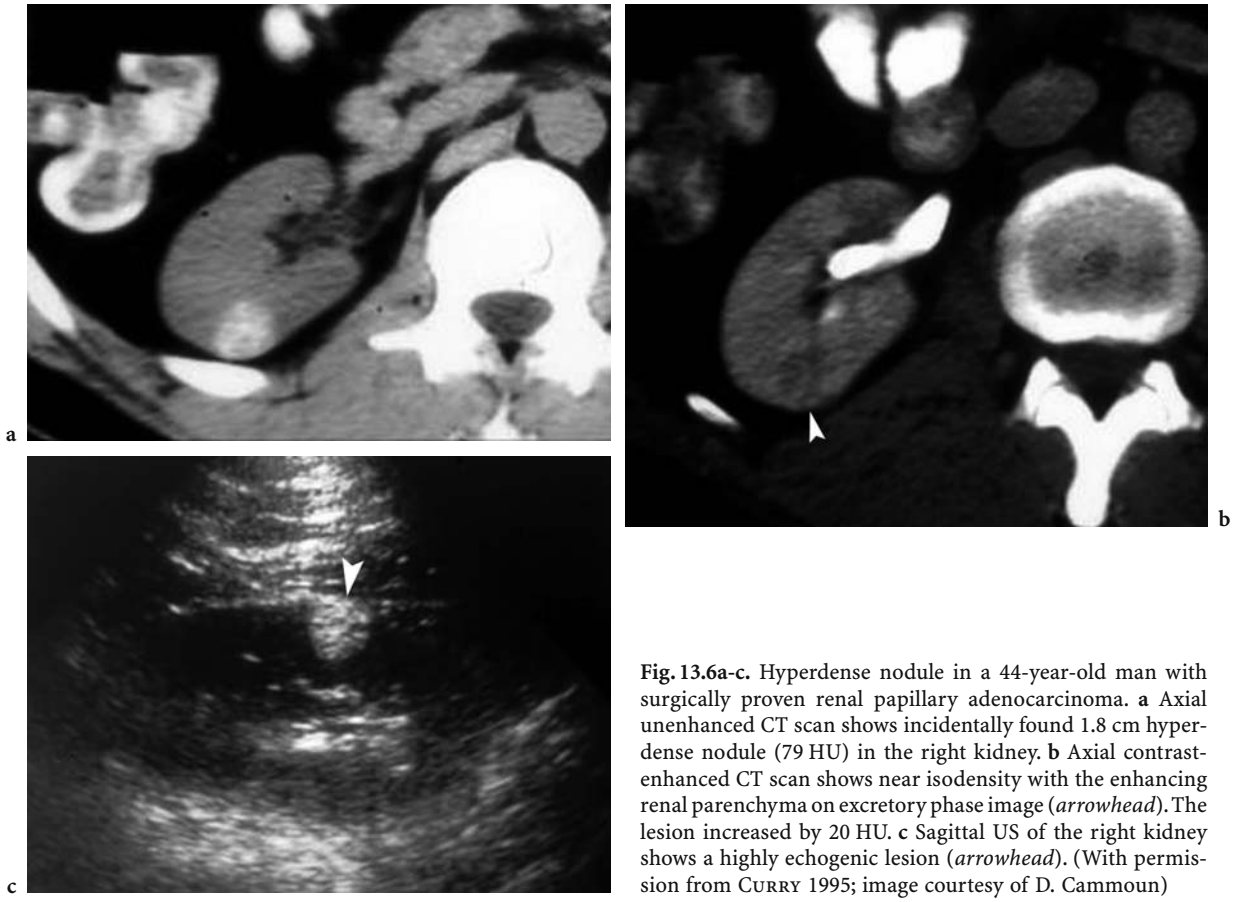

Fig. 13.6a-c. Hyperdense nodule in a 44-year-old man with surgically proven renal papillary adenocarcinoma. **a** Axial unenhanced CT scan shows incidentally found 1.8 cm hyperdense nodule (79 HU) in the right kidney. **b** Axial contrast-enhanced CT scan shows near isodensity with the enhancing renal parenchyma on excretory phase image (*arrowhead*). The lesion increased by 20 HU. **c** Sagittal US of the right kidney shows a highly echogenic lesion (*arrowhead*). (With permission from Curry 1995; image courtesy of D. Cammoun)

uting contrast material. If the lesion does not fully occupy the slice in the craniocaudal plane, the inclusion of normal parenchyma in the measured density will create a partial volume effect, i.e., pseudoenhancement.

Pseudoenhancement is usually not a problem with large renal masses whose visibility on multiple sequential images allow cursor readings precisely at the z-axis center. It is still a problem, however, when small masses appear on only a few contiguous axial images. An optimized CT technique is crucial in the evaluation of small renal masses. With current helical scanners, a maximum slice thickness of 5 mm should be used. Four-, 8-, and 16-slice multidetector scanners allow 2.5- to 1.25-mm sections. These sections are usually fused to 5-mm thickness for primary viewing, but indeterminate small lesions can often be resolved by creating overlapping 1.25-mm reconstructions (Fig. 13.10). In a recent report, multidetector CT images of kidneys scanned at 4×2.5-mm collimation were used to compare two types of reconstruction: 3 mm at 1.5-mm increments (with overlap) and the standard protocol of 5-mm thickness at 5-mm increments (without overlap). Twenty-eight additional lesions were detected using the thin-section overlapping protocol (Jinzaki et al. 2004).

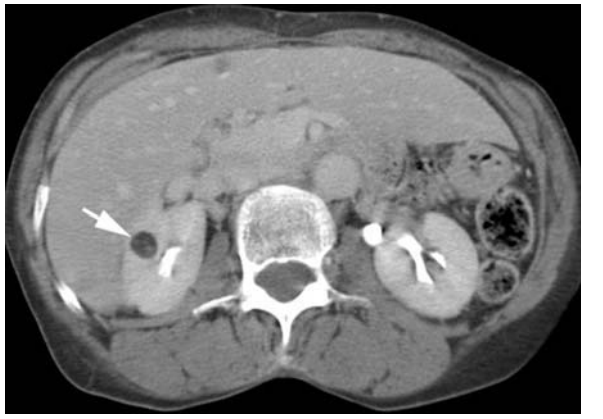

Fig. 13.7. Incidental small sporadic angiomyolipoma of the right kidney in a 69-year-old woman. Axial contrast-enhanced CT scan shows a lesion with very low density (–61 HU; *arrow*) consistent with macroscopic fat.

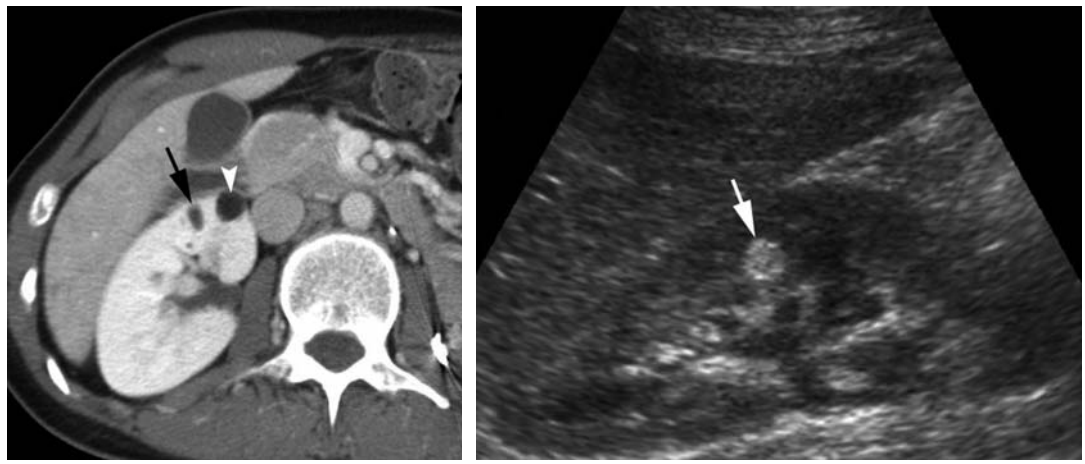

Fig. 13.8a,b. Tuberous sclerosis in a 37-year-old woman. **a** Axial contrast-enhanced CT scan shows two small (5 and 10 mm) angiomyolipomas of the right kidney that measured –70 HU (*arrow*) and –80 HU (*arrowhead*). **b** Sagittal ultrasound shows a hyperechoic 1-cm angiomyolipoma in another part of the same right kidney (*arrow*).

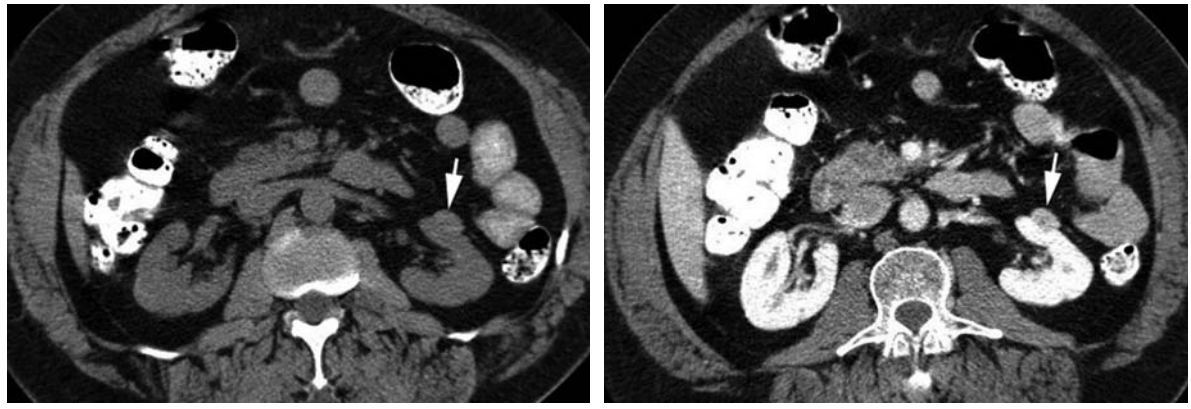

Fig. 13.9a,b. Angiomyolipoma without macroscopic fat in a 61-year-old woman. **a** Axial unenhanced CT scan shows a 1.7×1.4 cm exophytic lesion of the anterior left kidney (*arrow*). The lesion measures 66 HU. **b** Axial contrast-enhanced CT scan at the same level as **a** shows tumor enhancement to 103 HU (*arrow*). Laparoscopically resected tumor showed microscopic fat only.

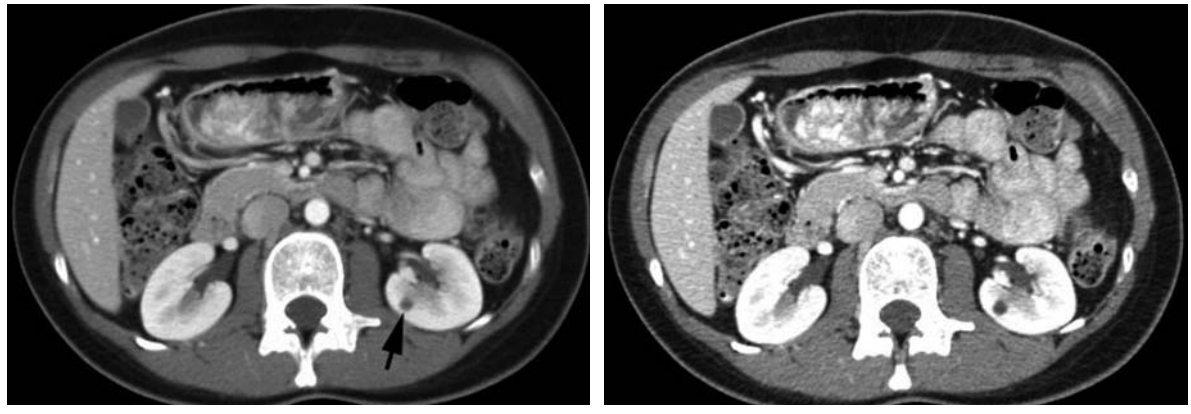

Fig. 13.10a,b. Simple cyst in a 42-year-old woman with breast cancer in whom an overlapping thin-section reconstruction on 16-slice MDCT was performed to evaluate an indeterminate small renal mass. **a** Axial contrast-enhanced CT scan shows 6 mm hypodensity in the left kidney (*arrow*) which measures 48 HU, not consistent with a simple cyst. **b** Axial 1.25-mm reconstructed CT image with repeat measurement of 6 HU confirms that the lesion is a cyst.

Despite the ability to create very thin sections, however, there is still a problem with pseudoenhancement in very small lesions in the range of 5–15 mm in diameter for both single-detector helical CT and multidetector scanners, both in vitro and in vivo (Bae et al. 2000; Birnbaum et al. 2002). A recent in vitro study suggests that the problem is greater with multidetector CT (MDCT), particularly those with matrix array detector design, and that the effect is more pronounced the smaller the lesion and the greater the surrounding enhancement (Abdulla et al. 2002). For cysts smaller than 1 cm in diameter, density differences of 12–33 HU can be seen at high background density. Scanning fluid-filled tubular phantoms, Abdulla et al. (2002) showed that the partial-volume effect was probably not responsible. They speculated that beam-hardening effects and differing reconstruction algorithms are responsible and suggested allowing a higher limit to the level of pseudoenhancement. Birnbaum et al. (2002) also suggest raising the threshold level of enhancement to 20 HU when characterizing lesions <1.5 cm. This approach would, however, reduce the sensitivity of the examination to detect hypovascular renal tumors. It is known that well-differentiated papillary RCCs show relatively low contrast enhancement because of their intrinsic hypovascularity (Herts et al. 2002; Jinzaki et al. 2000).

This element of uncertainty is reflected in a clinical study of interobserver variability in assessing lesions for enhancement, an effect most frequently observed for lesions in the range of 1.0–1.5 cm in size (Siegel et al. 1999). Jinzaki's study showed that with the use of MDCT and thin overlapping reconstructions, 84% (38 of 45) of masses between 5 and 10 mm could be characterized as cysts using the established contrast-enhanced threshold value of 20 HU (Jinzaki et al. 2000). Even this methodology has its limits, however. Although 5 mm and smaller lesions were detectable, most below that size could not be characterized.

13.4.3 Multiphasic CT Imaging

Another advantage of the development of multislice CT is the ability to image the kidneys in different physiologic stages of contrast excretion. There are several time-dependent post-contrast phases of enhancement which provide information germane to renal mass evaluation. The early arterial phase is reserved for cases in which surgical planning requires information on the number and location of vessels supplying the mass. The subsequent early cortical nephrogram phase exhibits well-defined corticomedullary differentiation with intense cortical opacification contrasting with the unopacified medulla. This is the phase commonly seen in CT studies of the abdomen in which the kidneys are not the primary focus. Thereafter, a uniform nephrogram phase develops as the medulla opacifies, and finally, an excretory phase occurs as the pyelocalyceal structures begin to fill with contrast.

The conspicuity of different types of renal tumor varies with the degree of vascularity and location in the parenchyma. Small hypovascular masses are difficult to discern in the early cortical phase unless they extend into the adjacent cortex (Fig. 13.11). Some small hypervascular tumors may enhance to

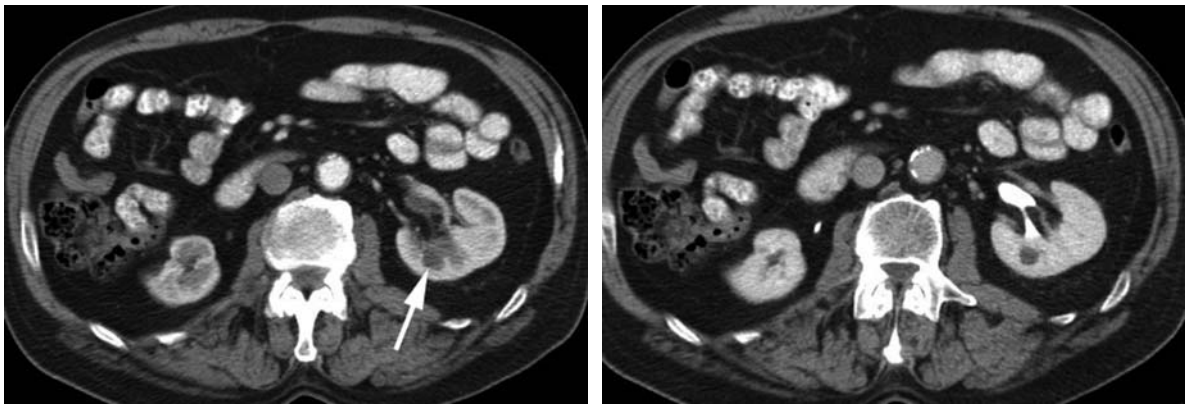

Fig. 13.11a,b. Conspicuity of small medullary masses on early vs later phase of excretion in a 47-year-old man undergoing CT for evaluation of hematuria. **a** Axial contrast-enhanced CT scan at early corticomedullary differentiation phase of contrast excretion shows 1 cm hypodensity in the posterior left kidney (*arrow*) which blends into the unopacified medulla. **b** The lesion is easily identified on excretory phase imaging and reconstructed thin sections determined it is a cyst.

the same degree as the opacified adjacent cortex, effectively camouflaging themselves from detection (Fig. 13.12). In end-stage kidneys with poor perfusion, however, small tumors may be more conspicuous since there is a higher achievable density difference between the tumor and diminished background parenchymal enhancement (Fig. 13.13; Takebayashi et al. 1999). Tumors with similar histology may exhibit differing enhancement characteristics depending on the degree of associated vascularity and necrosis (Fig. 13.14).

The excretory phase is most useful in the identification and staging of upper tract transitional cell carcinoma (Fig. 13.15). This tumor appears as a central area of high density in the renal pelvis or infundibulum on scans without contrast. After intravenous contrast, it exhibits only mildly increased density, corresponding to the hypovascular nature of these tumors. In the excretory phase transitional cell carcinoma creates solid or irregular filling defects in the expanded collecting system. Larger or infiltrative lesions may involve the adjacent parenchyma (Urban et al. 1997).

The phases of enhancement described above overlap and are variable in onset and duration depending on injection rate, volume of contrast used, and

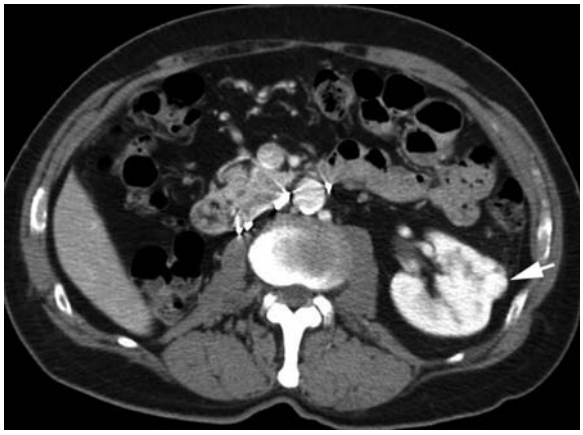

Fig. 13.12. Hypervascular mass difficult to discern on early phase of enhancement in a 79-year-old man. Axial contrast-enhanced CT scan shows intensely enhancing 1.8 cm mass (*arrow*), protruding from the lateral cortex of the left kidney, which nearly matches the adjacent normal renal cortex. Clear cell carcinoma treated by laparoscopic cryoablation.

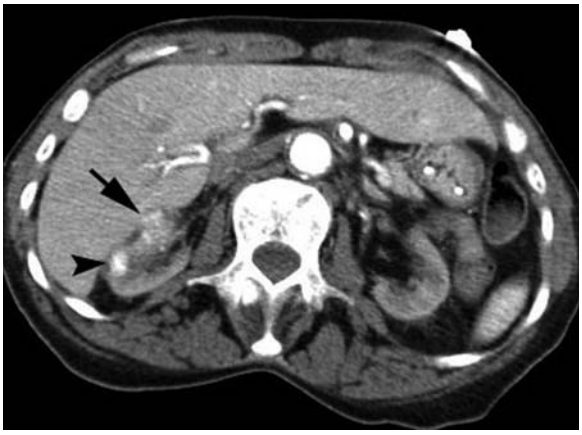

Fig. 13.13. Conspicuous hypervascular masses in a 66-year-old woman with end-stage renal disease. Axial contrast-enhanced CT scan at early arterial phase shows renal atrophy bilaterally with poor cortical perfusion. An intensely enhancing 9 mm nodule is present in the right kidney (*arrowhead*) with a larger, but less enhancing, lesion anterior to it (*arrow*).

a

b

Fig. 13.14a,b. End-stage renal disease in a 57-year-old woman on dialysis with hematuria. **a** Axial contrast-enhanced CT scan shows a homogeneously enhancing 7 mm nodule in the right upper pole (*arrow*). **b** Axial contrast-enhanced CT scan at mid-kidney level shows a heterogeneously enhancing nodule within a partially cystic mass posteriorly (*arrow*) and a poorly enhancing mass medially (*arrowhead*); all three were clear cell carcinomas. (With permission from Curry 2002)

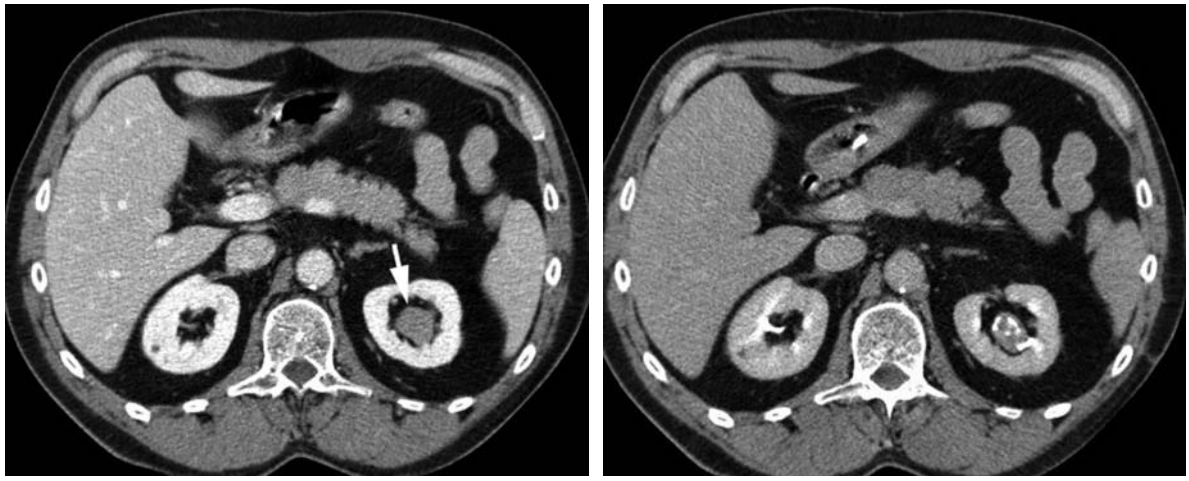

Fig. 13.15a,b. Transitional cell carcinoma in a 65-year-old man with gross painless hematuria. **a** Axial contrast-enhanced CT scan shows a central lesion in the left kidney (*arrow*) surrounded by renal sinus fat with density higher than urine (30 HU). **b** Excretory phase CT scan shows contrast filling interstices of tumor of the upper renal pelvis.

patient factors such as cardiac output. Probably the highest tumor detection yield is obtained when CT imaging is used in the homogeneous nephrographic phase (Silverman et al.1994; Szolar et al. 1997; Yuh and Cohan 1999).

13.4.4 CT Characteristics of Small Renal Masses

There is scant information on the CT features of small RCCs. In a review of CT features of 78 pathologically proven RCC tumors, eight were 3 cm in diameter or less (Zagoria et al. 1990); of these, one showed evidence of necrosis and one had distant metastases. The majority of small tumors in this series had a distinct tumor–parenchymal interface and none exhibited calcification. The authors therefore cautioned that small malignant renal tumors often have a benign appearance on incremental (non-helical) CT.

A Japanese study of 36 small RCC tumors compared cellular architecture with CT findings (Yamashita et al. 1992). The solid lesions (mostly clear cell carcinomas) were iso- or hypodense on unenhanced CT, whereas the papillary or tubular types (all granular cell) were iso- to slightly hyperdense (Fig. 13.6). Most of the tumors were homogeneous in appearance both before and after contrast, but 10 (28%) showed intratumoral necrosis, differing from Zagoria et al. (1990) study. Solid architecture tumors showed significantly higher contrast enhancement than the papillary or tubular tumors. Calcification was rare, occurring in only one tumor.

A later study retrospectively evaluated imaging characteristics of 35 renal masses under 3 cm in size obtained with more advanced helical CT techniques (Silverman et al. 1994). Twenty-seven of these masses proved to be RCC and the others were transitional cell carcinoma (2), leiomyoma (1), angiomyolipoma (1), and benign cysts (4). The findings were similar to incremental CT in that most of the small RCCs were non-calcified homogeneous masses which showed an initial density of 20 HU or greater and enhanced with contrast by at least 10 HU. Septations were underestimated in three cases and septate lesions were interpreted as solid in two cases. The authors concluded that many of the difficulties in the analysis of renal masses are not solved by helical CT imaging.

In 2000, a study of 40 surgically resected renal neoplasms evaluated enhancement patterns using a double-phase helical CT protocol (Jinzaki et al. 2000). The study found that the degree of enhancement in the corticomedullary differentiation phase correlated with microvessel density and that not all tumors with homogeneous enhancement showed necrosis or hemorrhage on histologic evaluation. Although enhancement patterns differed among the subtypes of RCC, with clear cell carcinomas showing greater peak enhancement in this phase than chromophobe or papillary RCC, it was not possible to differentiate benign oncocytomas from metanephric adenomas in the series. This result is not

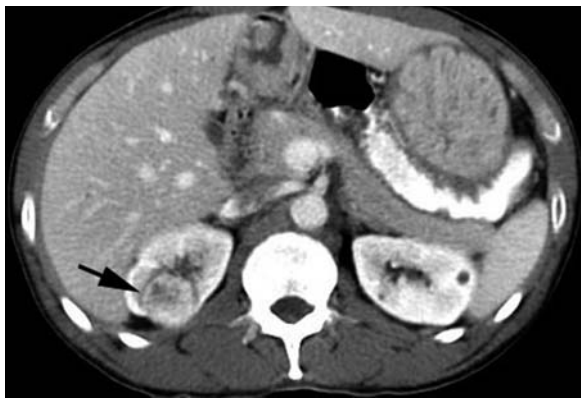

Fig. 13.16. Hypervascular tumor in a 54-year-old man. Axial contrast-enhanced CT scan shows 2.5 cm mass in the upper pole of the right kidney (*arrow*). Pathologist could not distinguish between oncocytoma or chromophobe RCC because the resected tumor had features supportive of both types of tumor.

surprising, given that it is difficult for pathologists to determine whether a neoplasm with oncocytic features is benign or malignant (Figs. 13.16, 13.17).

In a study on differentiation of subtypes of RCC using biphasic and monophasic helical CT, Kim et al. (2004) found that heterogeneous or predominantly peripheral enhancement was typical of small clear cell carcinomas, whereas most papillary and chromophobe tumor subtypes showed homogeneous enhancement.

Another 2004 study of renal masses evaluated with MDCT showed that the newer scanner technology and thin overlapping reconstructions make it easier to distinguish cysts, reducing the number of indeterminate small renal masses. It has not been proven, however, that solid lesions or cystic lesions with septa or nodularity <1 cm in size can be characterized (Jinzaki et al. 2004).

13.5 MR Imaging of Small Renal Masses

Magnetic resonance imaging was not used initially as the primary method of investigation of renal masses, in part because of limitations in detection with conventional spin-echo sequences. Since the signal intensity of solid tumors can resemble that of normal renal parenchyma on both T1- and T2-weighted images, there is only a 63% renal tumor detection rate at a size less than 3 cm in diameter (Semelka et al. 1991). This limitation, coupled with other factors such as slow scan times, limited availability and cost, initially restricted MR imaging to patients with renal failure and iodine or contrast sensitivity (Figs. 13.18, 13.19); however, recent advances in MR imaging with dynamic gadolinium enhancement, fat suppression, and surface coils, have made detection and characterization of small lesions possible (Fig. 13.20; Pretorius et al. 1999). In a retrospective review of MR imaging signal characteristics of 35 lesions of this size (20 RCCs and 15 benign lesions), enhancement made it simple to differentiate hypervascular RCCs from hypovascular tumors and benign lesions (Scialpi et al. 2000). Hypovascular tumors and benign lesions could not be distinguished, however, on simple observation and required quantitative evaluation of signal intensity profiles and contrast-to-noise ratios.

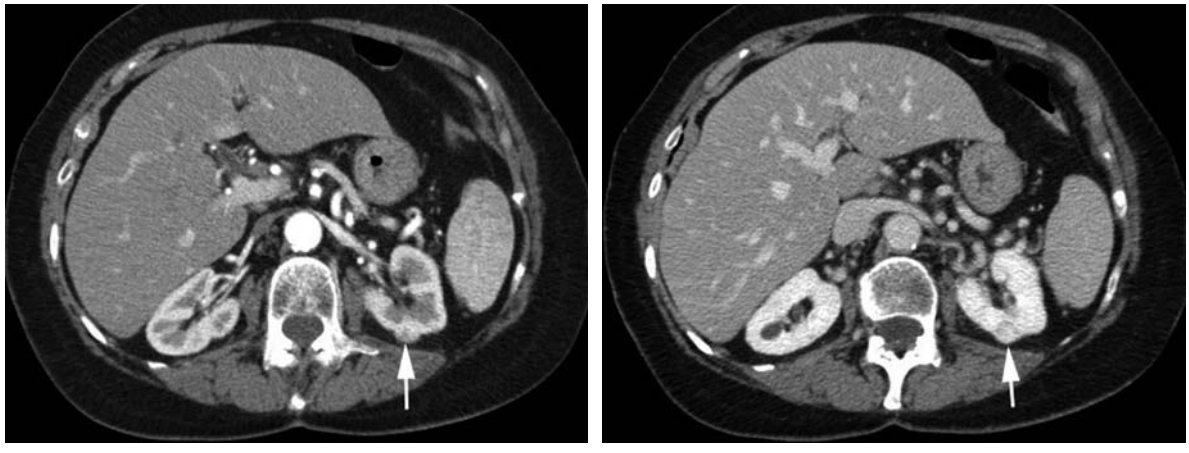

a b

Fig. 13.17a,b. Oncocytoma in a 75-year-old woman with history of breast carcinoma. **a** Axial contrast-enhanced CT scan at corticomedullary differentiation phase incidentally detects a 1.5 cm left renal mass (*arrow*). **b** This mass is better seen at nephrogram phase (*arrow*). Core biopsy pathology prior to radiofrequency ablation was consistent with oncocytoma rather than granular cell or chromophobe carcinoma.

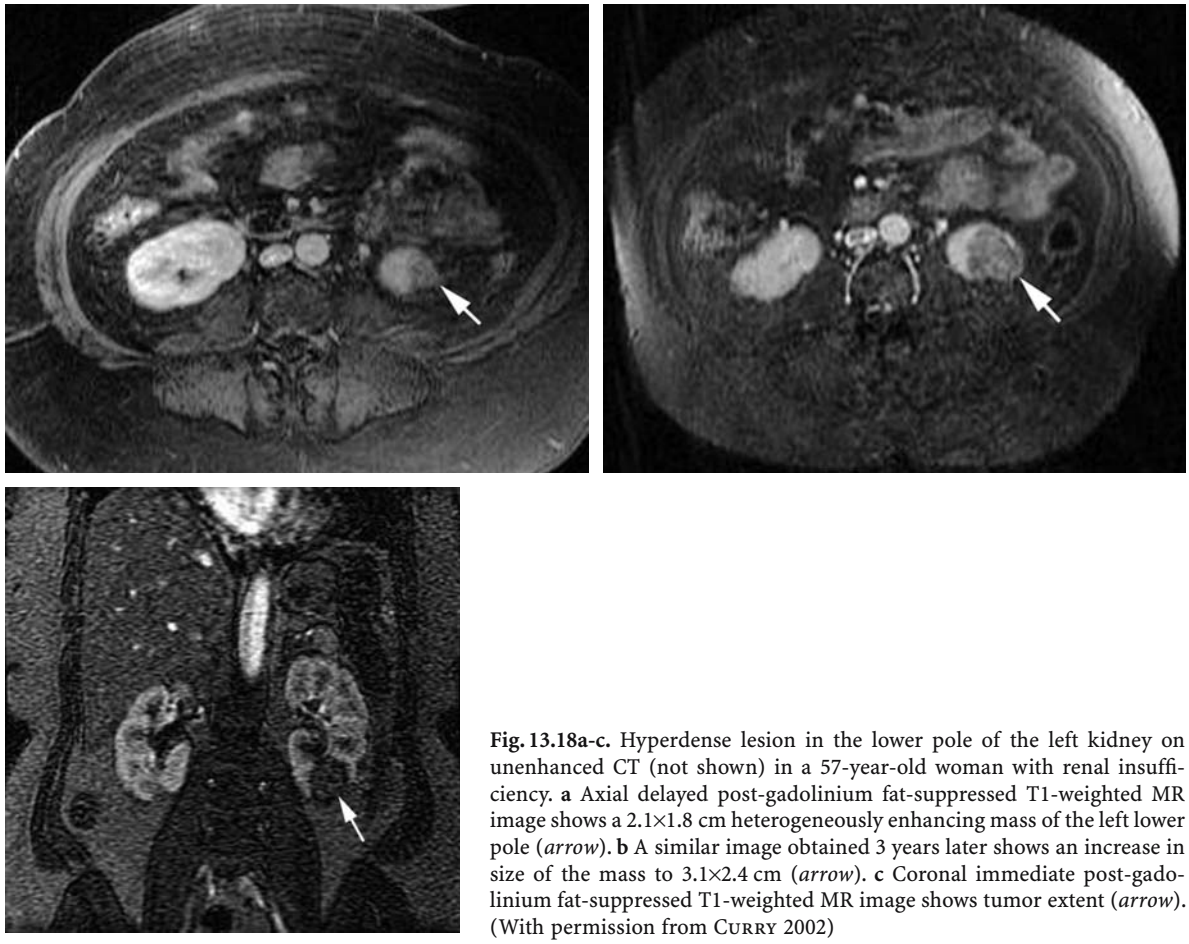

Fig. 13.18a-c. Hyperdense lesion in the lower pole of the left kidney on unenhanced CT (not shown) in a 57-year-old woman with renal insufficiency. **a** Axial delayed post-gadolinium fat-suppressed T1-weighted MR image shows a 2.1×1.8 cm heterogeneously enhancing mass of the left lower pole (*arrow*). **b** A similar image obtained 3 years later shows an increase in size of the mass to 3.1×2.4 cm (*arrow*). **c** Coronal immediate post-gadolinium fat-suppressed T1-weighted MR image shows tumor extent (*arrow*). (With permission from Curry 2002)

13.6 Ultrasound of Small Renal Masses

Ultrasound is less accurate in detecting and characterizing small renal neoplasms than CT or MR imaging. A study of 20 patients with von Hippel-Lindau disease, genetically predisposed to developing cysts and solid tumors of the kidney, showed that US was able to detect only 70% of lesions 2 cm in diameter, whereas CT detected 95% (Jamis-Dow et al. 1996). Size was a more important factor than cystic vs solid nature. Most RCCs are hypoechoic to normal renal parenchyma, but some are isoechoic and therefore undetectable unless they protrude significantly from the kidney surface. Nearly one-third of small RCC tumors are hyperechoic and may be mistaken for a benign AML (Fig. 13.6; Forman et al. 1993). In these cases the presence of an anechoic rim or central cystic areas are US features which suggest RCC over AML (Siegel et al. 1996).

13.7 Fine-Needle Aspiration and Biopsy of Small Renal Masses

Fine-needle aspiration and core biopsy are useful techniques in the evaluation of extrarenal tumors but are not routinely used in the kidney. Most studies show that imaging diagnosis is more accurate, and complications, although rare, such as hemorrhage, pneumothorax, or needle-tract seeding, may occur (Zagoria 2000). Fine-needle aspirates of small renal lesions may not yield enough tissue for definitive diagnosis and cellular heterogeneity and the potential for sampling error contribute to uncertainty (Campbell et al. 1997). Core biopsies do not yield any improved benefit in the kidney. A prospective series determining the accuracy of core biopsies of renal lesions obtained intraoperatively reported a false-negative rate of 20% and a false-positive rate of 34% (Dechet et al. 1999). A retrospective study of percu-

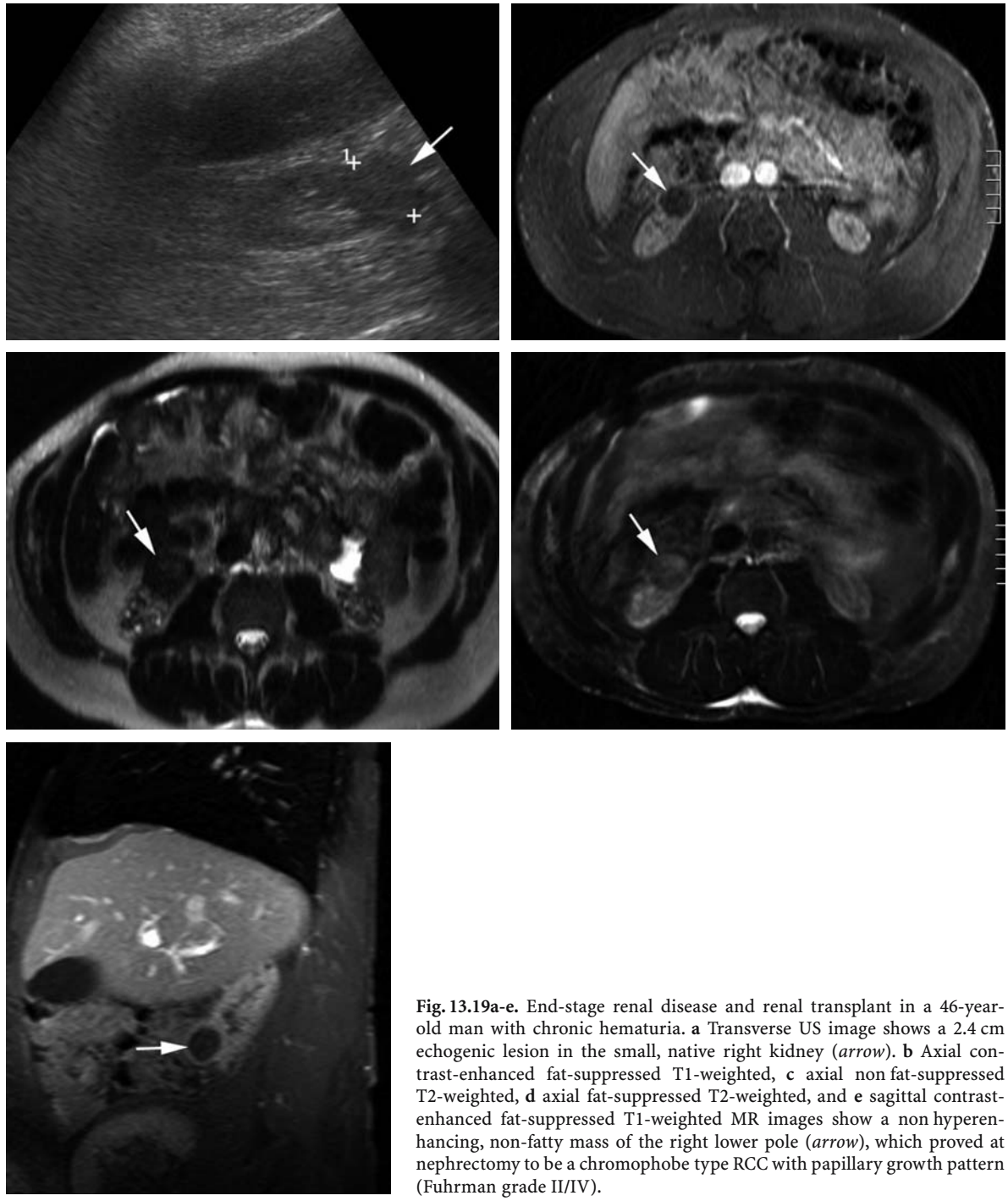

Fig. 13.19a-e. End-stage renal disease and renal transplant in a 46-year-old man with chronic hematuria. **a** Transverse US image shows a 2.4 cm echogenic lesion in the small, native right kidney (*arrow*). **b** Axial contrast-enhanced fat-suppressed T1-weighted, **c** axial non fat-suppressed T2-weighted, **d** axial fat-suppressed T2-weighted, and **e** sagittal contrast-enhanced fat-suppressed T1-weighted MR images show a non hyperenhancing, non-fatty mass of the right lower pole (*arrow*), which proved at nephrectomy to be a chromophobe type RCC with papillary growth pattern (Fuhrman grade II/IV).

taneous biopsies of renal masses showed that four of ten false-negative results for RCC occurred in lesions of 3 cm diameter or less (Rybicki et al. 2003).

There may, however, be a role for biopsy in the case of small lesions whose imaging evaluation is equivocal and in which the patient has been referred for percutaneous ablation of a presumed cancer. Since as many as 37% of patients referred for such treatment may have benign masses, biopsy may be appropriate to avoid an invasive procedure (Tuncali et al. 2004). Biopsy of renal masses is also appropriate in problem cases, such as the presence of a non-renal primary tumor or lymphoma where treatment decisions would be altered by the outcome (Figs. 13.21–13.24).

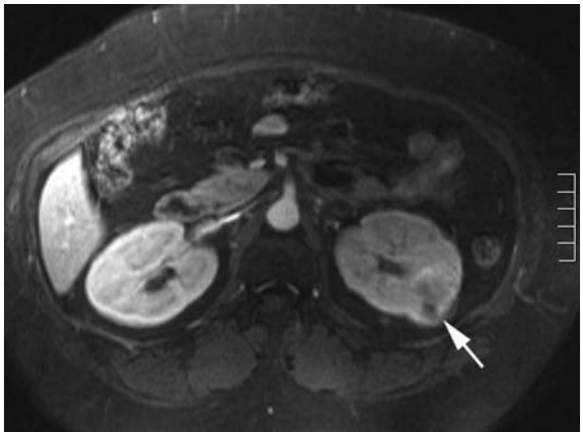

Fig. 13.20. Complex left upper pole renal lesion on ultrasound exam (not shown) in a 53-year-old woman with pancreatitis. Axial contrast-enhanced fat-suppressed T1-weighted MR image shows a 2.5 cm left heterogeneously enhancing mass which proved to be a Fuhrman grade III clear cell carcinoma at surgery (*arrow*).

Fig. 13.21. Renal cell carcinoma in a 51-year-old man with melanoma of the ear. Axial contrast-enhanced CT scan shows 1.9 cm tumor of the right kidney (*arrow*). Pathology yielded a clear cell carcinoma (Fuhrman grade I/IV).

a

b

Fig. 13.22a,b. Renal metastasis from small cell lung cancer in a 51-year-old man. **a** Initial axial contrast-enhanced CT scan shows solitary small right posterior renal mass (*arrow*). **b** Axial contrast-enhanced CT scan one month later shows the mass increased strikingly in size.

13.8 Treatment Options

Small renal neoplasms may be treated by wedge resection, partial nephrectomy, laparoscopic surgery, or percutaneous tumor ablation techniques such as cryotherapy and radiofrequency ablation. The percutaneous approaches reduce morbidity and convalescence time. They are still invasive procedures, however, and not all small renal neoplasms are destined to behave aggressively. If the object of surgery is to remove a tumor which is life threatening, there ought to be guidelines for selecting which lesions should be treated and which should undergo careful observation.

Is the detection of very small solid renal lesions of 1–1.5 cm size important? Does resection/ablation of neoplasms of this size lead to a cancer-free, longer life? These questions about the effect of discovery on mortality point to biases built into such speculation (Black and Ling 1990; Bosniak 1995). If the lesion is destined to grow slowly and the patient dies of unrelated causes, length of time bias is introduced. If the lesion is of questionable malignant potential, overdiagnosis bias exists. If very small lesions are by nature highly aggressive, and destined to end the patient's life, finding them earlier probably does not influence the ultimate outcome (lead-time bias).

Bosniak (1995) advocates observation for lesions less than 2 cm in diameter in patients who are

Fig. 13.23 Isolated renal lymphoma in a 71-year-old woman with abdominal pain. Axial contrast-enhanced CT scan shows a small left renal mass (*arrow*). The mass was percutaneously biopsied and was found to be B-cell non-Hodgkin lymphoma.

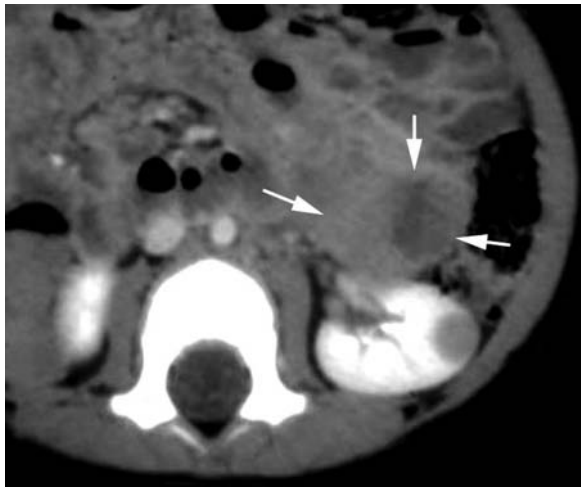

Fig. 13.24 Metastatic neuroblastoma in an 18-month-old boy presenting with leg pain. Axial contrast-enhanced CT scan shows an enhancing (83 HU) 1 cm solid lesion in the left kidney. A metastasis was present in the femur. The lower margin of an adrenal mass extends anterior to the kidney (*arrows*). Lesions were biopsy proven. (With permission from Curry 1995)

elderly or poor surgical risks. He would extend this to 2.5–3.0 cm during the observation period so that growth rate can be assessed periodically. He suggests follow-up studies at 6- to 12-month intervals, with the interval determined by growth rate. If the lesion is growing significantly and resection can be performed, surgery would then be justified. He warns, however, that observation should be reserved for homogeneous, well-defined, non-necrotic tumors, since necrotic tumors tend to be more aggressive. Observation is not justified in a young, healthy patient who is found to have a tumor of >1.5–2.0 cm. Although these masses may show indolent growth, they should be resected at discovery to avoid the risk that the lesion will grow rapidly and metastasize.

13.9 Conclusion

Radiologists frequently encounter small renal masses in daily practice. Most are small benign cysts which are difficult to characterize because of their size. With modern cross-sectional imaging techniques, however, it is possible to distinguish most of these from true renal neoplasms. The small renal neoplasms that contain fat or reside within the collecting system of the kidney are easily identified and managed appropriately. The remainder of enhancing, small solid renal masses continue to be a challenge. Since their histologic make-up and biologic behavior cannot be accurately predicted by imaging, a choice of nephron-sparing surgical or percutaneous ablation techniques vs "watchful waiting" are rational options for management. The appropriate course of action depends heavily on individual patient factors.

References

Abdulla C, Kalra MK, Saini S et al. (2002) Pseudoenhancement of simulated renal cysts in a phantom using different multidetector CT scanners. Am J Roentgenol 179:1473–1476

Aizawa S, Suzuki M, Kikuchi Y et al. (1987) Clinicopathological study on small renal cell carcinomas with metastases. Acta Pathol Jpn 37:947–954

Amendola MA, Bree RL, Pollack HM et al. (1988) Small renal cell carcinomas: resolving a diagnostic dilemma. Radiology 166:637–641

Bae KT, Heiken JP, Siegel CL et al. (2000) Renal cysts: Is attenuation artifactually increased on contrast-enhanced CT images? Radiology 216:792–796

Bell ET (ed) (1950) Tumors of the kidney. In: Renal diseases. Lea and Febiger, Philadelphia

Bennington JL (1973) Cancer of the kidney: etiology, epidemiology, and pathology. Cancer 32:1017–1029

Bennington JL (1987) Renal adenoma. World J Urol 5:66–70

Birnbaum BA, Maki DD, Chakraborty DP et al. (2002) Renal cyst pseudoenhancement evaluation with an anthropomorphic body CT phantom. Radiology 225:83–90

Black WC, Ling A (1990) Is earlier diagnosis really better? The misleading effects of lead time and length time biases. Am J Roentgenol 155:625–630

Bosniak MA (1995) Observation of small incidentally detected renal masses. Semin Urol Oncol 13:267–272

Bosniak MA, Rofsky NM (1996) Problems in the detection and characterization of small renal masses. Radiology 198:638–641

Bosniak MA, Birnbaum BA, Krinsky GA et al. (1995) Small renal parenchymal neoplasms: further observations on growth. Radiology 197:589–597

Campbell SC, Novick AC, Herts B et al. (1997) Prospective evaluation of fine needle aspiration of small, solid renal masses: accuracy and morbidity. Urology 50:25–29

Curry NS (1995) Small renal masses (lesions smaller than 3 cm): imaging evaluation and management. Am J Roentgenol 164:355–362

Curry NS (2002) Imaging the small solid renal mass. Abdom Imaging 27:629–636

Curry NS, Schabel, SI, Betsill WL (1986) Small renal neoplasms: diagnostic imaging, pathologic features, and clinical course. Radiology 158:113–117

Dechet CB, Sebo T, Farrow G et al. (1999) Prospective analysis of intraoperative frozen needle biopsy of solid renal masses in adults. J Urol 162:1282–1285

Ellis WJ, Bauer KD, Oyasu R et al. (1992) Flow cytometric analysis of small renal tumors. J Urol 148:1774–1777

Eschwege P, Saussine C, Steichen B et al. (1996) Radical nephrectomy for renal cell carcinoma 30 mm or less: long-term follow-up results. J Urol 155:1196–1199

Fielding JR, Visweswaran A, Silverman S et al. (1999) CT and ultrasound features of metanephric adenoma in adults with pathologic correlation. J Comput Assist Tomogr 23:441–444

Forman HP, Middleton WD, Melson GL et al. (1993) Hyperechoic renal cell carcinomas: increase in detection at US. Radiology 188:431–434

Hajdu SI, Thomas AG (1967) Renal cell carcinoma at autopsy. J Urol 97:978–982

Herts BR, Coll DM, Novick AC et al. (2002) Enhancement characteristics of papillary renal neoplasms revealed on triphasic helical CT of the kidneys. Am J Roentgenol 178:367–372

Hsu RM, Chan DY, Siegelman SS (2004) Small renal cell carcinomas: correlation of size with tumor stage, nuclear grade, and histologic subtype. Am J Roentgenol 182:551–557

Jamis-Dow CA, Choyke PL, Jennings SB et al. (1996) Small (≤3 cm) renal masses: detection with CT versus US and pathologic correlation. Radiology 198:785–788

Jinzaki M, Tanimoto A, Mukai M et al. (2000) Double-phase helical CT of small renal parenchymal neoplasms: correlation with pathologic findings and tumor angiogenesis. J Comput Assist Tomogr 24:835–842

Jinzaki M, McTavish JD, Zou KH et al. (2004) Evaluation of small (≤3 cm) renal masses with MDCT: benefits of thin overlapping reconstructions. Am J Roentgenol 183:223–228

Kim JJ, Kim TK, Han JA et al. (2004) Differentiation of subtypes of renal cell carcinoma on helical CT scans. Am J Roentgenol 178:1499–1506

Levine E, Huntrakoon M, Wetzel CH (1989) Small renal neoplasms: clinical pathologic and imaging features. Am J Roentgenol 153:69–73

Macari M, Bosniak MA (1999) Delayed CT to evaluate renal masses incidentally discovered at contrast-enhanced CT: demonstration of vascularity with deenhancement. Radiology 213:674–680

Petersen RO (1992) Kidney: neoplastic disorders. In: Petersen RO (ed) Urologic pathology. Lippincott, Philadelphia, p 77

Pretorius ES, Siegelman ES, Ramchandani P et al. (1999) Renal neoplasms amenable to partial nephrectomy: MR imaging. Radiology 212:28–34

Reis M, Faria V, Lindoro J et al. (1988) The small cystic and noncystic noninflammatory renal nodules: a postmortem study. J Urol 140:721–723

Rendon RA, Stanietzky N, Panzarella T et al. (2000) The natural history of small renal masses. J Urol 164:1143–1147

Rybicki FJ, Shu KM, Cibas ES et al. (2003) Percutaneous biopsy of renal masses: sensitivity and negative predictive value stratified by clinical setting and size of masses. Am J Roentgenol 180:1281–1287

Scialpi M, DiMaggio A, Midiri M et al. (2000) Small renal masses: assessment of lesion characterization and vascularity on dynamic contrast-enhanced MR imaging with fat suppression. Am J Roentgenol 175:751–757

Semelka RC, Hricak H, Stevens SK et al. (1991) Combined gadolinium-enhanced and fat saturation MR imaging of renal masses. Radiology 178:803–809

Siegel CL, Middleton WD, Teefey SA et al. (1996) Angiomyolipoma and renal cell carcinoma: US differentiation. Radiology 198:785–788

Siegel CL, Fisher AJ, Bennett HF (1999) Interobserver variability in determining enhancement of renal masses on helical CT. Am J Roentgenol 172:1207–1212

Silverman SG, Lee BY, Seltzer SE et al. (1994) Small (≤to 3 cm) renal masses: correlation of spiral CT features and pathologic findings. Am J Roentgenol 163:597–605

Smith SJ, Bosniak MA, Megibow AJ et al. (1989) Renal cell carcinoma: earlier discovery and increased detection. Radiology 170:699–703

Someren A, Zaatari GS, Campbell WG et al. (1989) Tumors of differentiated tubular epithelium: renal "adenoma" and adenocarcinoma. In: Someren A (ed) Urologic pathology with clinical and radiologic correlations. Macmillan, New York, pp 162–163

Steinberg AP, Lin CH, Matin S et al. (2003) Impact of tumor size on laparoscopic partial nephrectomy: analysis of 163 patients (Abstract). J Urol 169 (Suppl):174a

Szolar DH, Kammerhuber F, Altzieber S et al. (1997) Multiphasic helical CT of the kidney: increased conspicuity for detection and characterization of small (<3 cm) renal masses. Radiology 201:211–217

Takebayashi S, Hidai H, Chiba T et al. (1999) Using helical CT to evaluate renal cell carcinoma in patients undergoing hemodialysis: value of early enhanced images. Am J Roentgenol 172:429–433

Takebayashi S, Hidai H, Chiba T et al. (2000) Renal cell carcinoma in acquired cystic kidney disease: volume growth rate determined by helical computed tomography. Am J Kidney Dis 36:759–766

Talamo TS, Shonnard JW (1980) Small renal adenocarcinoma with metastases. J Urol 124:132–134

Tuncali K, van Sonnenberg E, Shankar S et al. (2004) Evaluation of patients referred for percutaneous ablation of renal tumors: importance of a preprocedural diagnosis. Am J Roentgenol 183:575–582

Urban BA, Buckley J, Soyer P et al. (1997) CT appearance of transitional cell carcinoma of the renal pelvis. Am J Roentgenol 169:157–168

Volpe A, Panzarella T, Rendon RA et al. (2004) The natural history of incidentally detected small renal masses. Cancer 100:738–745

Warshauer DM, McCarthy SM, Street L et al. (1988) Detection of renal masses: sensitivities and specificities of excretory urography/linear tomography, US and CT. Radiology 169:363–365

Yamashita Y, Takahashi M, Watanabe O et al. (1992) Small renal cell carcinoma: pathologic and radiologic correlation. Radiology 184:493–498

Yuh BI, Cohan RH (1999) Detecting and characterizing renal masses during helical CT. Am J Roentgenol 173:747–755

Zagoria RJ (2000) Imaging of small renal masses: a medical success story. Am J Roentgenol 175:945–955

Zagoria RJ, Wolfman NT, Karstaedt N et al. (1990) CT features of renal cell carcinoma with emphasis on relation to tumor size. Invest Radiol 25:261–266